Automated coordination corrected enthalpies with AFLOW-CCE

Rico Friedrich,[1,2,3] Marco Esters,[1,2] Corey Oses,[1,2] Stuart Ki,[1,2] Maxwell J. Brenner,[1,2]
David Hicks,[1,2] Michael J. Mehl,[1,2] Cormac Toher,[1,2] and Stefano Curtarolo[2,4]

[1] *Department of Mechanical Engineering and Materials Science, Duke University, Durham, North Carolina 27708, USA*
[2] *Center for Autonomous Materials Design, Duke University, Durham, North Carolina 27708, USA*
[3] *Institute of Ion Beam Physics and Materials Research, Helmholtz-Zentrum Dresden-Rossendorf, 01328 Dresden, Germany*
[4] *Materials Science, Electrical Engineering, Physics and Chemistry, Duke University, Durham NC, 27708, USA**

(Dated: February 2, 2022)

The computational design of materials with ionic bonds poses a critical challenge to thermodynamic modeling since density functional theory yields inaccurate predictions of their formation enthalpies. Progress requires leveraging physically insightful correction methods. The recently introduced coordination corrected enthalpies (CCE) method delivers accurate formation enthalpies with mean absolute errors close to room temperature thermal energy, *i.e.* ≈ 25 meV/atom. The CCE scheme, depending on the number of cation-anion bonds and oxidation state of the cation, requires an automated analysis of the system to determine and apply the correction. Here, we present AFLOW-CCE — our implementation of CCE into the AFLOW framework for computational materials design. It features a command line tool, a web interface and a Python environment. The workflow includes a structural analysis, automatically determines oxidation numbers, and accounts for temperature effects by parametrizing vibrational contributions to the formation enthalpy per bond.

Keywords: computational materials science, formation enthalpy, high-throughput computing

arXiv:2101.02724v2 [cond-mat.mtrl-sci] 12 Mar 2021

I. INTRODUCTION

Materials design of systems with ionic bonding contributions, *i.e.* compounds including elements of significantly different electronegativity, necessitates an accurate modelling of their thermodynamic stability [1–5]. The appropriate descriptor is the formation enthalpy [6] — the enthalpy difference between the compound and its elemental references, or its recursive factorization to study multicomponent systems [7]. For metals, high-throughput compatible (semi-)local density functional theory (DFT) is known to provide accurate results with errors significantly smaller than the thermal energy at room temperature (≈ 25 meV/atom) [8, 9]. This fueled the construction of large materials databases with millions of entries [10–18]. On the contrary, ionic materials pose a much more fundamental challenge for computational approaches.

As outlined in Ref. 1, the formation enthalpy can be subdivided into a total energy difference between the compound and the elements plus a (small) vibrational contribution due to zero-point and thermal effects. As long as all phases involved are chemically similar (in terms of their electronic delocalization character), standard (semi-)local DFT's systematic error cancellation allows for a good approximation of the total energy difference [8, 9]. This breaks down for ionic systems, such as oxides and nitrides [1–4, 19]: little error cancellation can be expected between an ionic compound and its metallic/diatomic-gaseous references. Consequently, computing reliable formation enthalpies *ab initio* would require accurate total energies for all systems involved. This is generally not possible within a (semi-)local approximation.

Significant efforts have been undertaken to investigate the accuracy that can be obtained from a specific level of theory. Many studies demonstrate that compared to experimental formation enthalpies [20–23], the typical mean absolute error (MAE) for standard functionals — such as LDA [24, 25] or PBE [26] — is on the order of several hundred meV/atom [1–4, 19, 27, 28]. For meta-generalized-gradient approximations, such as the Bayesian error estimation (mBEEF) [29] or the strongly constrained and appropriately normed (SCAN) [30] functionals, an MAE of about 100 meV/atom is obtained [1, 27, 28, 31]. While computationally more demanding, hybrid functionals yield only modest improvements over PBE for transition metal oxides and sulfides [32, 33]. Non-self-consistent exact exchange plus random phase approximation (EXX+RPA) and renormalized adiabatic PBE (rAPBE) calculations on PBE orbitals for small sets of about 20 oxides achieved MAEs down to 74-95 meV/atom [32, 34–36]. In conclusion, even for the most expensive DFT-based approaches, no satisfactory accuracy (≈ 25 meV/atom) is achieved. Preliminary tests for MgH_2 indicate that Quantum Monte Carlo can achieve accurate results with an error of ≈20 meV/atom [37, 38], although it remains to be determined whether this applies generally for all materials.

Physically motivated empirical correction schemes parametrizing (semi-)local DFT errors with respect to measured values are the only feasible option, achieving accurate formation enthalpies and enabling high-throughput materials design of ionic systems. Initially, a correction for the oxygen reference energy of 1.36 eV per O_2 for PBE was introduced [19]. This scheme was extended to other gases such as H_2, N_2, F_2, and Cl_2, as well as sulfides for several functionals [39, 40]. On top of this, for systems with transition metal ions, an approach for mixing GGA and GGA+U calculations was developed, reducing the MAE

* stefano@duke.edu

to 45 meV/atom for a test set of 49 ternary oxides [3]. Leveraging this method, extensive further parameterization within a local-environment dependent approach was found to lower the MAE to 19 meV/atom [41]. A drawback is, however, that non-transition metals remain uncorrected, which can be particularly problematic for heavy p-block elements [1]. As a complementary approach, the fitted elemental-phase reference energies (FERE) method introduces energy shifts for the elements on an equal footing to minimize the error between measured and calculated results for a large set of binary compounds [2, 4]. FERE values for many elements were calculated, yielding an MAE of 48 meV/atom when applied to a test set of 55 ternary compounds. Recently, correction schemes have also been extended to finite temperatures and the Gibbs free energies of solids [42]. It should be noted that the accuracy of schemes fitted to measured values is limited by the experimental error. In the supplementary information of our previous work [1], we investigated the deviation between measured values of different collections for a large set of oxides, indicating that the typical experimental error bar is on the order of 10-20 meV/atom.

While the above correction methods were a major step forward for materials design, their accuracy is limited and the relative stability of polymorphs — sometimes erroneously predicted by DFT [27] — cannot be corrected. Moreover, correction methods based on only composition can lead to incorrect thermodynamic behavior when considering activity *vs.* concentration [1]. To address these shortcomings, we have recently introduced a new universal method: coordination corrected enthalpies (CCE) [1]. This advanced correction scheme is the first to leverage structural information by assigning corrections per cation-anion bond, as well as considering the cation oxidation state. CCE achieves an MAE of 27 (24) meV/atom for a test set of 71 (7) ternary oxides (halides), on par with room temperature thermal energy ($\approx$ 25 meV/atom) [1]. It can also correct the relative stability at fixed composition and avoids incorrect thermodynamic behavior by construction.

Here, we present our automated implementation of CCE into the AFLOW framework for computational materials design. It identifies the number of cation-anion bonds, automatically determines oxidation numbers, and includes thermal effects by applying different corrections for designated temperatures. AFLOW-CCE includes a command line interface, a web application, and a Python environment providing useful tools for the scientific community to automatically calculate the CCE correction and formation enthalpies for a given input structure. The article is organized as follows: after introducing the computational details of the method, a short overview on the CCE functionality in AFLOW is given. Then, the specific analyses within the implementation are described including structural analysis, automatic determination of oxidation numbers, and the inclusion of temperature effects. Available options for the command line interface, CCE corrections for 0 K, and CCE@exp corrections for room temperature are discussed in details.

II. COMPUTATIONAL DETAILS

The *ab-initio* calculations for the exchange-correlation functionals LDA [24, 25], PBE [26] and SCAN [30] are performed with AFLOW [9, 43–47] and the Vienna *Ab-initio* Simulation Package (VASP) [48] with settings according to Refs. 1 and 49. Thermal contributions to the formation enthalpy are calculated using the quasi-harmonic Debye model implemented via the AFLOW-Automatic Gibbs Library (AGL) [50–52].

Using binary compounds $A_{x_1}Y_{x_2}$ as the fit set, the CCE corrections $\delta H^{T,A^{+\alpha}}_{A-Y}$ per cation-anion $A-Y$ bond and cation oxidation state $+\alpha$ are obtained from the difference between (zero-temperature and zero-pressure) DFT formation enthalpies and experimental standard formation enthalpies at temperature T [1]:

$$\Delta_{\rm f}E^{0,\rm DFT}_{A_{x_1}Y_{x_2}} - \Delta_{\rm f}H^{\circ,T,\rm exp}_{A_{x_1}Y_{x_2}} = x_1 N_{A-Y}\delta H^{T,A^{+\alpha}}_{A-Y}\,, \qquad (1)$$

where N_{A-Y} is the number of nearest neighbor $A-Y$ bonds and x_i are stoichiometries for the i-species. Standard conditions are indicated by the "$\circ$" superscript. T can be 298.15 or 0 K, *i.e.* temperature effects are included in the corrections. A detailed justification of this is presented later.

The corrections can then be applied to any multinary compound $A_{x_1}B_{x_2}\ldots Y_{x_n}$ to obtain the CCE formation enthalpy $\Delta_{\rm f}H^{\circ,T,\rm CCE}_{A_{x_1}B_{x_2}\ldots Y_{x_n}}$:

$$\Delta_{\rm f}H^{\circ,T,\rm CCE}_{A_{x_1}B_{x_2}\ldots Y_{x_n}} = \Delta_{\rm f}E^{0,\rm DFT}_{A_{x_1}B_{x_2}\ldots Y_{x_n}} - \sum_{i=1}^{n-1} x_i N_{i-Y}\delta H^{T,i^{+\alpha}}_{i-Y}\,, \qquad (2)$$

where N_{i-Y} is the number of nearest neighbor bonds between the cation i and anion Y-species. For multi-anion compounds [53], the corrections are summed for all anions separately in Eq. (2).

For the AFLOW-ICSD database, the CCE methodology is applied equivalently with the compound energies partly calculated within DFT+U [49]. In addition, composition dependent energy shifts are applied for the elements for which a U is used to align the related reference energies with the ones calculated from DFT+U.

The room temperature ($T_{\rm r}$ = 298.15 K) formation enthalpy CCE@exp [1] calculated from experimental formation enthalpies per bond $\delta H^{T_{\rm r},i^{+\alpha}}_{i-Y,\rm exp}$ is given by:

$$\Delta_{\rm f}H^{\circ,T_{\rm r},\rm CCE@exp}_{A_{x_1}B_{x_2}\ldots Y_{x_n}} = \sum_{i=1}^{n-1} x_i N_{i-Y}\delta H^{T_{\rm r},i^{+\alpha}}_{i-Y,\rm exp}. \qquad (3)$$

These values provide a rough guess with an estimated average accuracy of about 250 meV/atom as obtained from a test for ternary oxides [1].

III. RESULTS

The automated CCE implementation inside AFLOW enables the correction of an extensive library of ionic materials that are made available via the AFLOW APIs [59, 60] and web interfaces [10]. The implementation features three ways of user interaction depicted in Fig. 1: (i) a command line tool, (ii) a web application, and (iii) a Python environment. The command line tool (Fig. 1(a-f)) provides the CCE corrections and formation enthalpies, (automatically determined) oxidation numbers, and cation coordination numbers for the given structure file that can be in any format recognizable by AFLOW, such as VASP POSCAR [48], Quantum Espresso [54], FHI-AIMS [55], ABINIT [56], ELK [57] and CIF [58]. Available options are described in Section "CCE command line interface". The web interface (Fig. 1(g)) prints the cation coordination numbers, oxidation numbers and CCE corrections for the selected functionals using the given structure. The output also includes the CCE formation enthalpies when precalculated DFT values are entered in the designated fields. The Python environment is distributed with the AFLOW source and can be generated with the command `aflow --cce --print=python`. It connects to the command line functionality and imports the results into a `CCE` class similar to the Python modules of AFLOW-SYM [61] and AFLOW-CHULL [62]. An example script leveraging the functionality is depicted in Fig. 1(h). The CCE object has three built-in methods: `get_corrections(struct_file_path, functionals, enthalpies_formation_dft, oxidation_numbers)`, `get_oxidation_numbers(struct_file_path)`, and `get_cation_coordination_numbers(struct_file_path)` corresponding to the command line options mentioned in Section "CCE command line interface". Each method requires a path to the input structure file (`struct_file_path`). For `get_corrections`, providing `functionals`, DFT formation enthalpies (`enthalpies_formation_dft`), and input `oxidation_numbers` for all atoms in the structure, are optional arguments. The results are returned in the form of a Python dictionary.

CCE command line interface

`aflow --cce`

- Prints instructions and example input structure.

`aflow --cce=STRUCTURE_FILE_PATH`

- Prints the results of the full CCE analysis, *i.e.* cation coordination numbers, oxidation numbers, and CCE corrections and formation enthalpies, for the given structure. STRUCTURE_FILE_PATH is the path to the structure file. The file can be in any format supported by AFLOW, *e.g.* VASP POSCAR, QUANTUM ESPRESSO, AIMS, ABINIT, ELK and CIF. For VASP, a VASP5 POSCAR is required or, if a VASP4 POSCAR is used, the species must be written on the right side next to the coordinates for each atom just as for the example input structure obtained from `--cce`.

`aflow --get_cce_corrections < STRUCTURE_FILE_PATH`

- Determines the CCE corrections and formation enthalpies for the structure in file STRUCTURE_FILE_PATH.

`aflow --get_oxidation_number < STRUCTURE_FILE_PATH`

- Determines the oxidation numbers for the structure in file STRUCTURE_FILE_PATH.

`aflow --get_cation_coord_num < STRUCTURE_FILE_PATH`

- Determines the number of anion neighbors for each cation for the structure in file STRUCTURE_FILE_PATH.

Options for `--cce=STRUCTURE_FILE_PATH` and `--get_cce_corrections < STRUCTURE_FILE_PATH`:

`--enthalpies_formation_dft=enth_1,enth_2,...`

- `enth_1,enth_2,...` is a comma separated list for precalculated DFT formation enthalpies. They are assumed to be: (i) negative for compounds lower in enthalpy than the elements, (ii) in eV/cell. Currently, corrections are available for PBE, LDA, and SCAN.

`--functionals=func_1,func_2,func_3`

- `func_1,func_2,func_3` is a comma separated list of functionals for which corrections should be returned. If used together with `--enthalpies_formation_dft`, the functionals must be in the same sequence as the DFT formation enthalpies they correspond to. Available functionals are: (i) PBE, (ii) LDA, and (iii) SCAN. Default: PBE (if only one DFT formation enthalpy is provided).

`--oxidation_numbers=ox_num_1,ox_num_2,...`

- `ox_num_1,ox_num_2,...` is a comma separated list of oxidation numbers. It is assumed that: (i) one is provided for each atom of the structure and (ii) they are in the same sequence as the corresponding atoms in the provided structure file.

General option

`--print=out|json`

- Obtains output in table format (`--print=out`) or as JSON (`--print=json`). Default: `out`.

Structural analysis. For evaluating the number of cation-anion bonds (cation coordination numbers), first the (main) anion species of the system is determined as

a

```
aflow --get_cce_corrections < test.POSCAR --enthalpies_formation_dft=-63.452,-72.084,-72.412 --functionals=PBE,LDA,SCAN
```

b

CCE CORRECTIONS:

functional	temperature (K)	correction (eV/cell)	correction (eV/atom)
PBE	298.15	+5.954	+0.298
PBE	0	+5.538	+0.277
LDA	298.15	−3.377	−0.169
LDA	0	−3.836	−0.192
SCAN	298.15	−3.678	−0.184
SCAN	0	−4.124	−0.206

CCE FORMATION ENTHALPIES:

functional	temperature (K)	form. enthalpy (eV/cell)	form. enthalpy (eV/atom)
PBE	298.15	−69.406	−3.470
PBE	0	−68.990	−3.449
LDA	298.15	−68.707	−3.435
LDA	0	−68.248	−3.412
SCAN	298.15	−68.734	−3.437
SCAN	0	−68.288	−3.414
CCE@exp	298.15	−74.230	−3.711

c

```
aflow --get_oxidation_numbers < test.POSCAR
```

d

atom	species	oxidation state
1	Ca	+2
2	Ca	+2
3	Ca	+2
4	Ca	+2
5	O	−2
6	O	−2
7	O	−2
8	O	−2
9	O	−2
10	O	−2
11	O	−2
12	O	−2
13	O	−2
14	O	−2
15	O	−2
16	O	−2
17	Ti	+4
18	Ti	+4
19	Ti	+4
20	Ti	+4

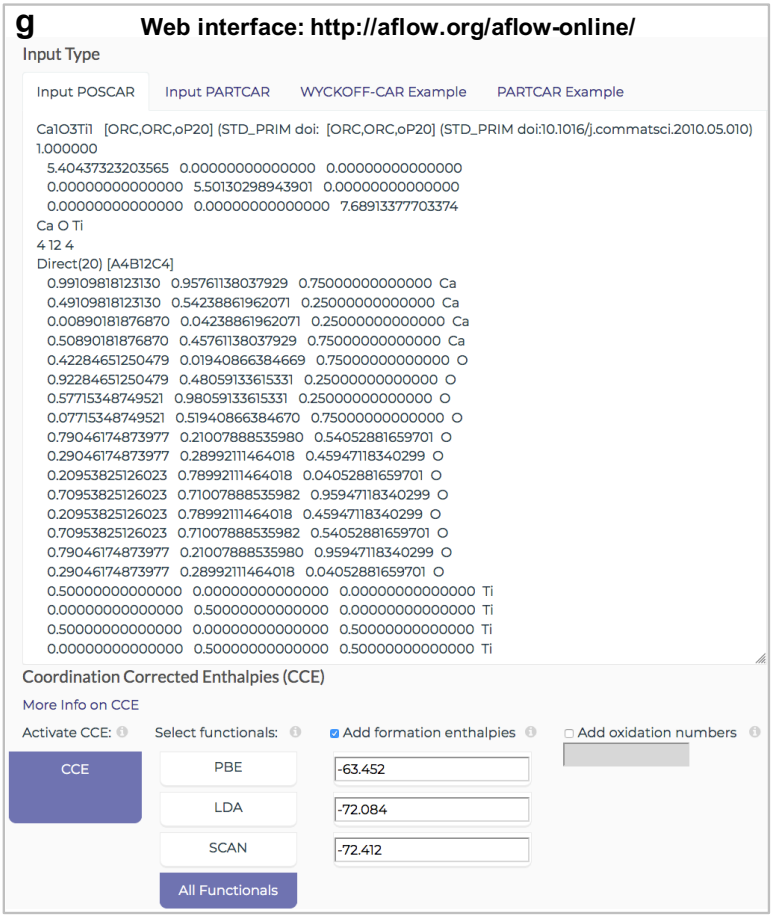
e

```
aflow --get_cation_coord_nums < test.POSCAR
```

f

atom	species	anion	coord. number
1	Ca	O	8
2	Ca	O	8
3	Ca	O	8
4	Ca	O	8
17	Ti	O	6
18	Ti	O	6
19	Ti	O	6
20	Ti	O	6

g



h

```python
from aflow_cce_python import CCE
from pprint import pprint

struct_file_path = "test.POSCAR"
functionals = "PBE,LDA,SCAN"
enthalpies_formation_dft = [-63.452,-72.084,-72.412]
oxidation_numbers = [2,2,2,2,-2,-2,-2,-2,-2,-2,-2,-2,-
    ↪ 2,-2,-2,-2,4,4,4,4]

cce = CCE(aflow_executable='./aflow')
output = cce.get_corrections(struct_file_path,
    ↪ functionals=functionals, enthalpies_formation_dft
    ↪ =enthalpies_formation_dft, oxidation_numbers=
    ↪ oxidation_numbers)
pprint(output)
```

FIG. 1. **User interfaces.** (**a**) Example command — here for perovskite $CaTiO_3$ — for the AFLOW-CCE command line tool. The input structure file (here test.POSCAR), precalculated DFT formation enthalpies per cell, and functionals are given via the options `--get_cce_corrections < test.POSCAR`, `--enthalpies_formation_dft=-63.452,-72.084,-72.412`, and `--functionals=PBE,LDA,SCAN`, respectively. The structure can be in any format recognizable by AFLOW, such as VASP POSCAR [48], Quantum Espresso [54], FHI-AIMS [55], ABINIT [56], ELK [57] and CIF [58]. Oxidation numbers for all atoms can be provided as a comma separated list as input using `--oxidation_numbers=ox_num_1,ox_num_2,...`. (**b**) When executed, the output includes the CCE corrections and formation enthalpies at both 298.15 and 0 K. If no DFT formation enthalpies are given, an estimate for the formation enthalpy at 298.15 K based on experimental values per bond (CCE@exp, blue) [1] is calculated according to Eq. (3). (**c/d**) Example command/output when determining oxidation numbers for the structure in test.POSCAR. (**e/f**) Example command/output when determining cation coordination numbers for the structure in test.POSCAR. (**g**) The web interface yields the cation coordination numbers, oxidation numbers, and CCE corrections for the structure provided in the field "Input POSCAR". If DFT formation enthalpies per cell are provided, the output also includes the CCE formation enthalpies. (**h**) Example Python script using the AFLOW-CCE Python environment. Similar to the command line, `functionals`, `enthalpies_formation_dft`, and input `oxidation_numbers` are optional arguments for the `get_corrections` method. The results are returned as a dictionary.

the one with the highest Allen electronegativity (EN) [63–65]. A check is performed whether the material is a multi-anion system [53], *i.e.* whether atoms of a type other than the main anion species are only bound to atoms of lower EN or its own type. If such atoms are found, they are designated as additional anions. This is for instance the case for N in $HfTaNO_3$, where O is the main anion. Note that in some compounds certain species can occur both as anion and as cation: in ammonium-nitrate (NH_4NO_3) for instance, N occurs both in -3 and $+5$ oxidation states depending on its neighbors.

Subsequently, the number of anion neighbors for each cation is determined. For this bonding analysis, the nearest neighbor distance is obtained for each species. A bonding cutoff is set by adding a tolerance of 0.5 Å in accordance with Ref. 1. Then, all anion neighbors between the species selective minimum distance and the cutoff are counted. For the multi-anion analysis, the tolerance is reduced to 0.4 Å since for larger values, different anions of systems known to be multi-anion compounds would be detected as being bonded. For instance, in $HfTaNO_3$, if the tolerance is not reduced, N and O would be detected as being neighbors and hence nitrogen would not be identified as an anion.

When oxygen is found as an anion, the O-O distances in the system are determined to detect per- and superoxides. The following scenarios can occur: (i) the O-O bond is longer than 1.6 Å indicating an oxide (O^{2-} ion), (ii) the bond length is between 1.4 and 1.6 Å (peroxide), (iii) the bond length lies between 1.3 and 1.4 Å, (superoxide), and (iv) the bond length is shorter than 1.3 Å, *i.e.* the structure may contain molecular oxygen the enthalpy of which is not correctable within CCE. For certain special cases such as alkali metal sesquioxides, several of the above scenarios can be fulfilled simultaneously and the implementation will then treat the system as incorporating multiple different oxygen ions. The separation of the different oxide types by bond length is based on the study of the relaxed structures of Li_2O_2, Na_2O_2, K_2O_2, SrO_2, BaO_2 (peroxides), NaO_2, KO_2, CsO_2 (superoxides), and O_2 [1]. The number of (su-)peroxide bonds is determined as half the number of (su-)peroxide O atoms.

Determination of oxidation numbers. The default method to automatically determine oxidation numbers is based on Allen ENs [63–65]. This choice is in accordance with International Union of Pure and Applied Chemistry (IUPAC) recommendations [68, 69] and also conforms with our own tests that this EN scale yields the most reliable oxidation numbers when compared to other scales such as Refs. 67 and 70. Table I lists the EN values together with the preferred and all known oxidation numbers for the elements according to Ref. 66, along with a few additions deemed necessary during the test of the implementation. The separation into preferred and all known oxidation numbers is motivated by the finding that in compounds with more than two species, elements tend to occur only in the preferred oxidation states [1]. Missing oxidation states will be added in future releases as needed.

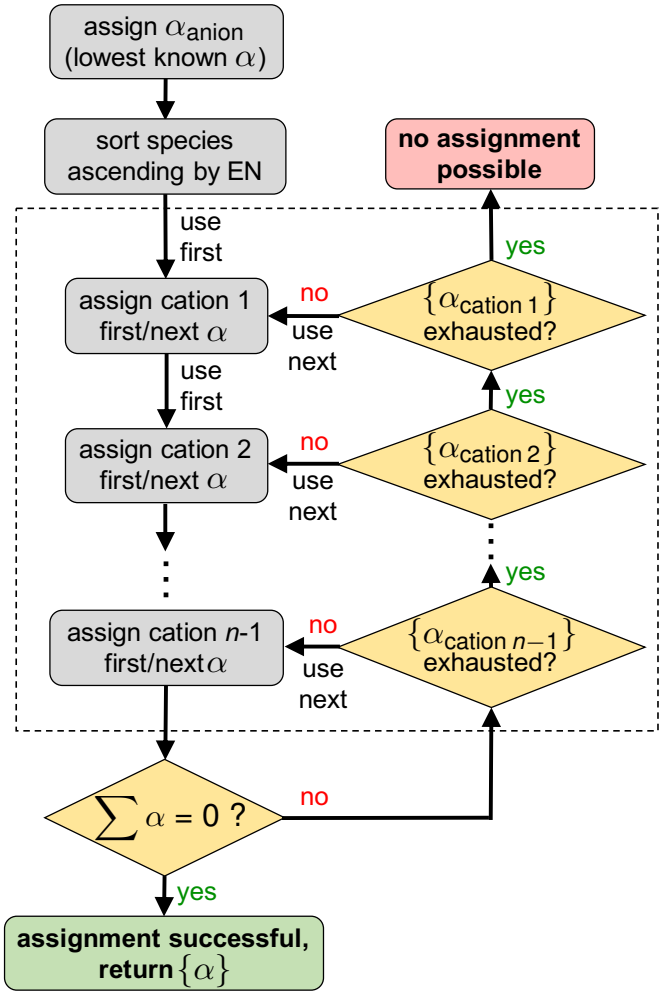


FIG. 2. **Oxidation number algorithm.** Schematic representation of the algorithm to determine oxidation numbers α of a compound with n-species. The part of the algorithm for determining cation oxidation numbers (inside the black dashed box) is first applied making use of the preferred oxidation numbers for all species. If no successful assignment is achieved, it is employed a second time after checking for mixed-valence compounds using all known oxidation states (Table I). The oxidation numbers of more electronegative cation species are iterated faster than the more electropositive ones. Three dots indicate proceeding equivalently for all further cation species. For multi-anion systems, atoms identified as additional anions during the structural analysis are excluded when assigning cation oxidation numbers.

The algorithm (Fig. 2) starts by assigning the anion oxidation numbers. For all anion atoms (main anion species and anions from multi-anion analysis) the lowest (most negative) oxidation number known for this species is assigned. If the atom was found to belong to a peroxide (superoxide) ion in the structural analysis, the oxidation number is changed to -1 (-0.5).

The set of possible cation oxidation states is first re-

TABLE I. **Electronegativities and oxidation numbers.** Allen ENs [63–65], as well as preferred and all known oxidation numbers according to Ref. 66 with additions, used in the CCE implementation. For Cr, the most preferred value is listed first.

element	Allen EN	oxidation numbers preferred	oxidation numbers all	element	Allen EN	oxidation numbers preferred	oxidation numbers all
H	2.3	+1	+1,−1	Rh	1.56	+3,+1	+5,+4,+3,+2,+1,0
He	4.16	-	-	Pd	1.58	+2	+4,+2,0
Li	0.912	+1	+1	Ag	1.87	+1	+2,+1
Be	1.576	+2	+2	Cd	1.52	+2	+2
B	2.051	+3	+3	In	1.656	+3	+3
C	2.544	+4,−4	+4,+2,−4	Sn	1.824	+4,+2	+4,+2
N	3.066	−3	+5,+4,+3,+2,−3	Sb	1.984	+3	+5,+3,−3
O	3.61	−2	−0.5,−1,−2	Te	2.158	+4	+6,+4,−2
F	4.193	−1	−1	I	2.359	−1	+7,+5,+1,−1
Ne	4.787	-	-	Xe	2.582	-	+8,+6,+4,+2
Na	0.869	+1	+1	Cs	0.659	+1	+1
Mg	1.293	+2	+2	Ba	0.881	+2	+2
Al	1.613	+3	+3	La[a]	1.09	+3	+3
Si	1.916	+4	+4,−4	Ce[a]	1.09	+3	+4,+3
P	2.253	+5	+5,+3,−3	Pr[a]	1.09	+3	+4,+3
S	2.589	+6	+6,+4,+2,−2	Nd[a]	1.09	+3	+3
Cl	2.869	−1	+7,+5,+3,+1,−1	Pm[a]	1.09	+3	+3
Ar	3.242	-	-	Sm[a]	1.09	+3	+3,+2
K	0.734	+1	+1	Eu[a]	1.09	+3	+3,+2
Ca	1.034	+2	+2	Gd[a]	1.09	+3	+3
Sc	1.19	+3	+3	Tb[a]	1.09	+3	+4,+3
Ti	1.38	+4	+4,+3,+2	Dy[a]	1.09	+3	+3
V	1.53	+5	+5,+4,+3,+2,0	Ho[a]	1.09	+3	+3
Cr	1.65	+3,+6	+6,+3,+2,0	Er[a]	1.09	+3	+3
Mn	1.75	+2	+7,+6,+4,+3,+2,0,−1	Tm[a]	1.09	+3	+3,+2
Fe	1.8	+3,+2	+6,+3,+2,0,−2	Yb[a]	1.09	+3	+3,+2
Co	1.84	+2	+3,+2,0,−1	Lu	1.09	+3	+3
Ni	1.88	+2	+3,+2,0	Hf	1.16	+4	+4,+3
Cu	1.85	+2,+1	+2,+1	Ta	1.34	+5	+5,+3
Zn	1.59	+2	+2	W	1.47	+6	+6,+5,+4,+3,+2,0
Ga	1.756	+3	+3	Re	1.6	+7	+7,+6,+4,+2,−1
Ge	1.994	+4	+4	Os	1.65	+4	+8,+6,+4,+3,+2,0,−2
As	2.211	+3	+5,+3,−3	Ir	1.68	+4,+1	+6,+4,+3,+2,+1,0,−1
Se	2.424	+4	+6,+4,−2	Pt	1.72	+4,+2	+4,+2,0
Br	2.685	−1	+7,+5,+3,+1,−1	Au	1.92	+3	+3,+1
Kr	2.966	+2	+2	Hg	1.76	+2	+2,+1
Rb	0.706	+1	+1	Tl	1.789	+1	+3,+1
Sr	0.963	+2	+2	Pb	1.854	+2	+4,+2
Y	1.12	+3	+3	Bi	2.01	+3	+5,+3
Zr	1.32	+4	+4,+3	Po	2.19	+4	+6,+4,+2
Nb	1.41	+5	+5,+3,+2	At	2.39	−1	+7,+5,+3,+1,−1
Mo	1.47	+6	+6,+5,+4,+3,+2,0	Rn	2.6	+2	+2
Tc	1.51	+7	+7	Fr	0.67	+1	+1
Ru	1.54	+4,+3	+8,+6,+4,+3,+2,0,−2	Ra	0.89	+2	+2

[a] Since there are no available Allen electronegativities for La-Yb, the value for Lu is used as these elements are usually very similar. This is confirmed by the Allred and Rochow electronegativities that are very similar for all lanthanides [67].

stricted to the preferred values for each species. All cations are then assigned the first (usually most positive) preferred oxidation number for their species. The only exception is Cr for which +3 is the first choice (Table I). After this initial assignment, the sum over all oxidation numbers is evaluated and — if it is zero — the assignment is considered successful. Otherwise, the algorithm proceeds by changing the preferred oxidation numbers according to EN: while checking the sum for each choice, the oxidation states of more electronegative (higher EN) cation species are changed to the next preferred value before the more electropositive (lower EN) ones. It is expected that more electropositive elements occur in higher oxidation states.

If all EN-directed choices of preferred oxidation numbers are exhausted without successful assignment, the system is checked for mixed-valence. For these special cases, the oxidation numbers are set explicitly. Currently, this

scenario includes Sb_2O_4, Pb_3O_4, Fe_3O_4, Mn_3O_4, Co_3O_4, Ti-O Magnéli phases, and alkali-metal sesquioxides. If still no successful assignment is achieved, the part of the algorithm for determining cation oxidation numbers (inside the black dashed box in Fig. 2) is repeated with all known oxidation numbers for all cation species. The scheme has been successfully tested on a large number of compounds, including oxides, fluorides, chlorides, and nitrides. The algorithm might not be particularly suited for organic compounds for which the oxidation state of C depends on the functional group. Such materials are presently beyond the scope of AFLOW-CCE.

For oxides, the oxidation numbers can also be determined from Bader charges [71], which are compared to the averaged template values of the binary fit set for the respective functional. The formal oxidation number is assigned according to the closest template value. However, this scheme shows systematic difficulties in assigning the correct oxidation numbers for several species in certain oxidation states such as Ti^{4+}, V^{5+}, Fe^{2+} and Fe^{3+}, for which error handling procedures have been implemented. This method is only invoked when specifically requested via the setting `DEFAULT_CCE_OX_METHOD=2` in the `.aflow.rc` setup file of AFLOW.

Finally, the user can also provide the oxidation numbers for all atoms as a comma separated list as input (option `--oxidation_numbers=` in the Section "CCE command line interface").

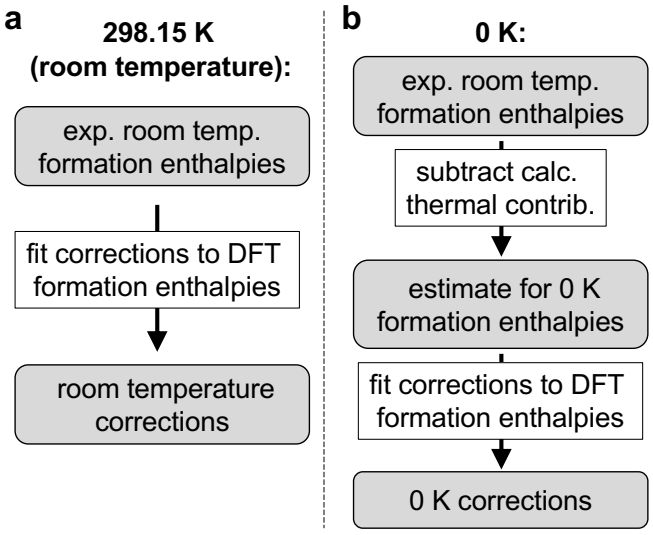


FIG. 3. **Corrections for different temperatures.** (**a**) For 298.15 K, the CCE corrections to the DFT formation enthalpies are fitted to experimental room temperature formation enthalpies resulting in room temperature corrections. (**b**) For 0 K, first the thermal contribution deduced from a quasi-harmonic Debye model [51] is subtracted from experimental values, resulting in estimates for 0 K formation enthalpies. CCE corrections fitted to these values yield 0 K corrections.

Inclusion of temperature effects. After the determination of the oxidation numbers, the cation-anion and cation oxidation state specific CCE corrections per bond $\delta H_{A-Y}^{T,A^{+\alpha}}$ (Eq. (1)) can be assigned. As outlined in Ref. 1, vibrational (zero-point and thermal) contributions to the formation enthalpy do not need to be calculated explicitly since they can be parameterized per bond and thus implicitly included into the corrections. Compared to when the vibrational contribution was explicitly included for the fit and test sets, the MAE of the corrected results increased by at most 1 meV/atom. This is negligible considering that the CCE MAE is on the order of 30 meV/atom. Temperature effects are thus included in the corrections according to Fig. 3(a): The CCE corrections to DFT formation enthalpies are fitted to experimental room temperature formation enthalpies resulting in room temperature corrections. When these are applied according to Eq. (2), a direct estimate of the room temperature formation enthalpy is obtained.

For 0 K (Fig. 3(b)), one first subtracts the calculated thermal contribution, deduced from a quasi-harmonic Debye model [51] according to Ref. [1], from the experimental formation enthalpy for each functional. This gives a good estimate for the (experimental) 0 K formation enthalpy. Then, the CCE corrections to the DFT formation enthalpies are fitted to these values yielding 0 K corrections. The approach does not capture any phase change of the elemental references from 0 K to room temperature. However, this is a rare event that occurs on an energy scale *below* room temperature, which is smaller than the CCE error.

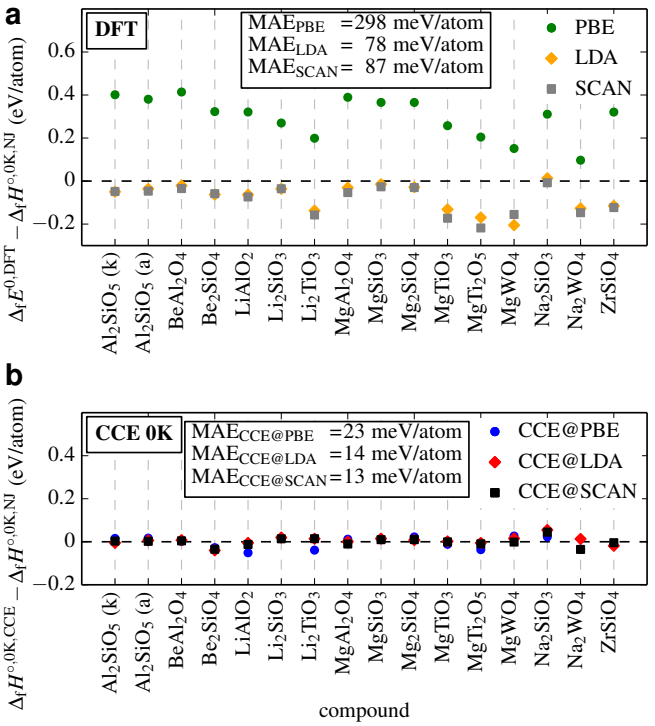


FIG. 4. **Validating 0 K predictions.** Deviations of (**a**) DFT formation enthalpies and (**b**) CCE 0 K predictions from experimental 0 K formation enthalpies from NIST-JANAF [21]. For Al_2SiO_5, the results for both the kyanite (k) and andalusite (a) structures are depicted.

To test the accuracy of the predicted 0 K formation enthalpies, they are compared to available tabulated values. Figure 4(a) shows the deviations between plain DFT results and 0 K formation enthalpies from the NIST-JANAF (NJ) thermochemical tables [21] for 16 ternary oxides. Typical large errors are indicated by the MAEs of 298, 78 and 87 meV/atom for PBE, LDA and SCAN, respectively. When corrected by CCE, the DFT results are drastically improved (Fig. 4(b)) with mean errors reduced to 23, 14 and 13 meV/atom, validating our 0 K approach.

As a future development, the temperature dependence can be implemented as a continuous variable, since it can be parameterized per bond and the thermal contributions at any temperature can be computed from the quasiharmonic Debye model [51] for the fit set. This ansatz, and other approaches directly targeting the Gibbs free energy [42] to include finite temperature effects, pave the way to move beyond stability predictions based only on enthalpies, which are crucial for *e.g.* high-entropy materials [72, 73].

The corrections are finally used to calculate the total CCE corrections and the CCE formation enthalpies according to Eq. (2) for 298.15 and 0 K for all functionals selected. If needed, corrections for (su-)peroxides are added according to Ref. [1] with the number of respective O-O bonds obtained from the structural analysis. If no precalculated DFT formation enthalpies are provided, an estimate for the formation enthalpy at 298.15 K based on experimental values per bond (CCE@exp) [1] is calculated according to Eq. (3).

TABLE II: **CCE corrections at 0 K for oxides.** Corrections per bond $\delta H_{A-Y}^{0\mathrm{K},A^{+\alpha}}$ of the CCE method for each cation species A in oxidation states $+\alpha$ for 0 K obtained from binary oxides. The corrections for Si and Ti in oxidation state +4 are obtained from α-quartz (AFLOW label `A2B_hP9_152_c_a` [74, 75]) and rutile (AFLOW label `A2B_tP6_136_f_a` [74, 75]), respectively. The corrections in the last line are for (su-)peroxides according to the approach outlined in Ref. 1. All corrections are in eV/bond.

cation species A	$+\alpha$	$\delta H_{A-Y}^{0\mathrm{K},A^{+\alpha}}$ PBE	LDA	SCAN	cation species A	$+\alpha$	$\delta H_{A-Y}^{0\mathrm{K},A^{+\alpha}}$ PBE	LDA	SCAN
Li	+1	0.0704	−0.0223	−0.0186	Sr	+2	0.1048	−0.0232	−0.0193
Be	+2	0.1875	0.0000	−0.0023	Y	+3	0.1304	−0.0280	−0.0543
B	+3	0.1825	−0.0835	−0.0612	Zr	+4	0.1320	−0.0530	−0.0709
Na	+1	0.0776	−0.0096	−0.0168	Nb	+2	0.0533	−0.1328	−0.0910
Mg	+2	0.1272	−0.0042	−0.0090	Mo	+4	0.0215	−0.1927	−0.1137
Al	+3	0.1778	−0.0168	−0.0222	Mo	+6	−0.0603	−0.3575	−0.2718
Si (α-qua.)	+4	0.2380	−0.0390	−0.0368	Ru	+4	−0.0115	−0.2133	−0.1192
K	+1	0.0803	−0.0301	−0.0071	Rh	+3	0.0065	−0.1415	−0.0631
Ca	+2	0.1002	−0.0395	−0.0280	Pd	+2	0.0548	−0.0830	−0.0280
Sc	+3	0.1541	−0.0166	−0.0338	Ag	+1	−0.0070	−0.0538	−0.0645
Ti	+2	0.1067	−0.0738	−0.0331	Cd	+2	0.1013	0.0130	0.0023
Ti	+3	0.0905	−0.0936	−0.0767	In	+3	0.1303	−0.0222	−0.0186
Ti (rut.)	+4	0.0972	−0.1072	−0.1345	Sn	+2	0.0650	−0.0665	−0.0158
V	+2	0.2620	0.1152	0.1547	Sn	+4	0.1433	−0.0540	−0.0237
V	+3	0.0918	−0.0734	−0.0600	Sb	+3	0.1153	−0.1212	−0.0267
V	+4	0.0375	−0.1598	−0.1637	Sb	+5	0.0970	−0.1418	−0.0669
V	+5	−0.0189	−0.2248	−0.2307	Te	+4	0.0558	−0.2123	−0.0970
Cr	+6	−0.1443	−0.3210	−0.2968	Cs	+1	0.1008	−0.0583	−0.0060
Cr	+3	0.1473	0.0391	−0.0247	Ba	+2	0.1165	0.0075	0.0020
Mn	+2	0.2513	0.2693	−0.0340	Hf	+4	0.1566	−0.0353	−0.0326
Mn	+4	0.0523	−0.1030	−0.1667	W	+4	0.0512	−0.1648	−0.0543
Fe	+2	0.1728	0.1287	0.0143	W	+6	−0.0025	−0.2165	−0.1448
Fe	+3	0.1586	0.0055	−0.0718	Re	+4	0.0845	−0.1302	0.0155
Co	+2	0.2373	0.1645	0.1193	Re	+6	−0.0803	−0.3125	−0.1682
Ni	+2	0.2537	0.1512	0.1955	Os	+4	0.0570	−0.1498	−0.0040
Cu	+1	0.1295	0.0318	0.0618	Os	+8	−0.2295	−0.3920	−0.2880
Cu	+2	0.0973	−0.0308	0.0020	Ir	+4	0.0157	−0.1868	0.0135
Zn	+2	0.1803	0.0368	0.0398	Hg	+2	0.1525	−0.0865	0.0380
Ga	+3	0.1925	−0.0022	0.0289	Tl	+1	−0.0053	−0.0660	−0.0605
Ge	+4	0.1895	−0.0462	0.0290	Tl	+3	0.0518	−0.0962	−0.0166
As	+5	0.1919	−0.0752	0.0092	Pb	+2	0.0033	−0.1093	−0.0550
Se	+4	0.0657	−0.2397	−0.1083	Pb	+4	0.0545	−0.1285	−0.0283
Rb	+1	0.0940	−0.0235	0.0031	Bi	+3	−0.0276	−0.1778	−0.0379
O	−1	−0.0856	−0.1110	0.2476	O	$-\frac{1}{2}$	−0.5435	−0.2697	−0.0468

TABLE III: **CCE@exp corrections at 298.15 K for oxides.** Corrections per bond $\delta H^{298.15\mathrm{K},A^{+\alpha}}_{A-Y,\mathrm{exp}}$ of the CCE@exp method for each cation species A in oxidation states $+\alpha$ for 298.15 K obtained from binary oxides. The corrections for Si and Ti in oxidation state +4 are obtained from α-quartz (AFLOW label `A2B_hP9_152_c_a` [74, 75]) and rutile (AFLOW label `A2B_tP6_136_f_a` [74, 75]), respectively. The corrections in the last line are for (su-)peroxides according to the approach outlined in Ref. 1. All corrections are in eV/bond.

cation species A	$+\alpha$	$\delta H^{298.15\mathrm{K},A^{+\alpha}}_{A-Y,\mathrm{exp}}$	cation species A	$+\alpha$	$\delta H^{298.15\mathrm{K},A^{+\alpha}}_{A-Y,\mathrm{exp}}$	cation species A	$+\alpha$	$\delta H^{298.15\mathrm{K},A^{+\alpha}}_{A-Y,\mathrm{exp}}$
Li	+1	−0.7746	Fe	+3	−0.7112	In	+3	−0.7997
Be	+2	−1.5790	Co	+2	−0.4107	Sn	+2	−0.7405
B	+3	−2.1998	Ni	+2	−0.4140	Sn	+4	−1.0033
Na	+1	−0.5415	Cu	+1	−0.4423	Sb	+3	−1.2370
Mg	+2	−1.0392	Cu	+2	−0.4043	Sb	+5	−0.8394
Al	+3	−1.4473	Zn	+2	−0.9083	Te	+4	−0.8380
Si (α-qua.)	+4	−2.3603	Ga	+3	−1.1288	Cs	+1	−0.5977
K	+1	−0.4705	Ge	+4	−1.0018	Ba	+2	−0.9468
Ca	+2	−1.0967	As	+5	−0.9536	Hf	+4	−1.6949
Sc	+3	−1.6482	Se	+4	−0.7777	W	+4	−1.0183
Ti	+2	−1.1719	Rb	+1	−0.4390	W	+6	−1.4557
Ti	+3	−1.3136	Sr	+2	−1.0227	Re	+4	−0.7755
Ti (rut.)	+4	−1.6307	Y	+3	−1.6453	Re	+6	−1.0177
V	+2	−0.7458	Zr	+4	−1.6249	Os	+4	−0.5088
V	+3	−1.0527	Nb	+2	−1.0875	Os	+8	−1.0200
V	+4	−1.2330	Mo	+4	−1.0155	Ir	+4	−0.4192
V	+5	−1.6067	Mo	+6	−1.9308	Hg	+2	−0.4705
Cr	+3	−0.9800	Ru	+4	−0.5268	Tl	+1	−0.2892
Cr	+6	−1.5210	Rh	+3	−0.3072	Tl	+3	−0.3372
Mn	+2	−0.6648	Pd	+2	−0.2993	Pb	+2	−0.5685
Mn	+4	−0.8998	Ag	+1	−0.0805	Pb	+4	−0.4742
Fe	+2	−0.4700	Cd	+2	−0.4463	Bi	+3	−0.5915
O	−1	2.7256	O	$-\frac{1}{2}$	1.7560			

IV. CONCLUSIONS

We have presented our implementation of the coordination corrected enthalpies (CCE) method into AFLOW for automated correction of DFT formation enthalpies. AFLOW-CCE provides a universal tool to obtain highly accurate formation enthalpies for ionic materials with a typical mean absolute error close to the room temperature thermal energy, *i.e.* ≈ 25 meV/atom [1]. It interoperates with the existing functionality of AFLOW and features a command line tool, a web interface, and a Python environment. Additionally, the AFLOW-CHULL module will be updated with the CCE formation enthalpies where appropriate [62].

The AFLOW-CCE workflow includes a structural analysis to identify the number of cation-anion bonds, an automatic determination of oxidation numbers based on Allen electronegativities, and the inclusion of temperature effects by parametrizing vibrational contributions to the formation enthalpy per bond.

With all the required functionality in place, the implementation will be extended to other anion classes beyond oxides such as nitrides, halides, and sulfides by adding the needed corrections in the near future.

V. CODE AVAILABILITY

The Automated CCE module is integrated into the AFLOW software (version 3.2.7 and later). The source code is available at http://aflow.org/install-aflow/ and http://materials.duke.edu/AFLOW/, and it is compatible with most Linux, macOS, and Microsoft operating systems. The CCE web tool is accessible via: http://aflow.org/aflow-online/. Tutorials are available through the AFLOW-School: http://aflow.org/aflow-school/. Questions and bug reports should be emailed to `aflow@groups.io` with a subject line containing "CCE".

ACKNOWLEDGMENTS

We thank Arkady Krasheninnikov, Demet Usanmaz, Frisco Rose, Eric Gossett, Denise Ford, Andriy Smolyanyuk, and Xiomara Campilongo for fruitful discussions. The authors acknowledge support by DOD-ONR (N00014-16-1-2326, N00014-17-1-2090, N00014-17-1-2876), and by the National Science Foundation under DMREF Grant No. DMR-1921909. R.F. acknowledges support from the Alexander von Humboldt foundation under the Feodor Lynen research fellowship.

[1] R. Friedrich, D. Usanmaz, C. Oses, A. Supka, M. Fornari, M. Buongiorno Nardelli, C. Toher, and S. Curtarolo, *Coordination corrected ab initio formation enthalpies*, npj Comput. Mater. **5**, 59 (2019).

[2] S. Lany, *Semiconductor thermochemistry in density functional calculations*, Phys. Rev. B **78**, 245207 (2008).

[3] A. Jain, G. Hautier, S. P. Ong, C. J. Moore, C. C. Fischer, K. A. Persson, and G. Ceder, *Formation enthalpies by mixing GGA and GGA+U calculations*, Phys. Rev. B **84**, 045115 (2011).

[4] V. Stevanović, S. Lany, X. Zhang, and A. Zunger, *Correcting density functional theory for accurate predictions of compound enthalpies of formation: Fitted elemental-phase reference energies*, Phys. Rev. B **85**, 115104 (2012).

[5] G. S. Rohrer *et al.*, *Challenges in Ceramic Science: A Report from the Workshop on Emerging Research Areas in Ceramic Science*, J. Am. Ceram. Soc. **95**, 3699–3712 (2012).

[6] G. L. W. Hart, S. Curtarolo, T. B. Massalski, and O. Levy, *Comprehensive Search for New Phases and Compounds in Binary Alloy Systems Based on Platinum-Group Metals, Using a Computational First-Principles Approach*, Phys. Rev. X **3**, 041035 (2013).

[7] C. Toher, C. Oses, D. Hicks, and S. Curtarolo, *Unavoidable disorder and entropy in multi-component systems*, npj Comput. Mater. **5**, 69 (2019).

[8] C. Wolverton and V. Ozoliņš, *First-principles aluminum database: Energetics of binary Al alloys and compounds*, Phys. Rev. B **73**, 144104 (2006).

[9] O. Levy, R. V. Chepulskii, G. L. W. Hart, and S. Curtarolo, *The New Face of Rhodium Alloys: Revealing Ordered Structures from First Principles*, J. Am. Chem. Soc. **132**, 833–837 (2010).

[10] S. Curtarolo, W. Setyawan, S. Wang, J. Xue, K. Yang, R. H. Taylor, L. J. Nelson, G. L. W. Hart, S. Sanvito, M. Buongiorno Nardelli, N. Mingo, and O. Levy, *AFLOWLIB.ORG: A distributed materials properties repository from high-throughput ab initio calculations*, Comput. Mater. Sci. **58**, 227–235 (2012).

[11] C. Oses, C. Toher, and S. Curtarolo, *Data-driven design of inorganic materials with the Automatic Flow Framework for Materials Discovery*, MRS Bull. **43**, 670–675 (2018).

[12] A. Jain, G. Hautier, C. J. Moore, S. P. Ong, C. C. Fischer, T. Mueller, K. A. Persson, and G. Ceder, *A high-throughput infrastructure for density functional theory calculations*, Comput. Mater. Sci. **50**, 2295–2310 (2011).

[13] J. E. Saal, S. Kirklin, M. Aykol, B. Meredig, and C. Wolverton, *Materials Design and Discovery with High-Throughput Density Functional Theory: The Open Quantum Materials Database (OQMD)*, JOM **65**, 1501–1509 (2013).

[14] S. Kirklin, J. E. Saal, B. Meredig, A. Thompson, J. W. Doak, M. Aykol, S. Rühl, and C. Wolverton, *The Open Quantum Materials Database (OQMD): assessing the accuracy of DFT formation energies*, npj Comput. Mater. **1**, 15010 (2015).

[15] C. Draxl and M. Scheffler, *NOMAD: The FAIR concept for big data-driven materials science*, MRS Bull. **43**, 676–682 (2018).

[16] S. R. Bahn and K. W. Jacobsen, *An object-oriented scripting interface to a legacy electronic structure code*, Comput. Sci. Eng. **4**, 56–66 (2002).

[17] D. D. Landis, J. S. Hummelshøj, S. Nestorov, J. Greeley, M. Dułak, T. Bligaard, J. K. Nørskov, and K. W. Jacobsen, *The Computational Materials Repository*, Comput. Sci. Eng. **14**, 51–57 (2012).

[18] G. Pizzi, A. Cepellotti, R. Sabatini, N. Marzari, and B. Kozinsky, *AiiDA: automated interactive infrastructure and database for computational science*, Comput. Mater. Sci. **111**, 218–230 (2016).

[19] L. Wang, T. Maxisch, and G. Ceder, *Oxidation energies of transition metal oxides within the GGA+U framework*, Phys. Rev. B **73**, 195107 (2006).

[20] O. Kubaschewski, C. B. Alcock, and P. J. Spencer, *Materials Thermochemistry* (Pergamon Press, Oxford, UK, 1993), 6th edn.

[21] M. W. Chase, Jr., *NIST-JANAF Thermochemical Tables* (American Chemical Society and American Institute of Physics for the National Institute of Standards and Technology, Woodbury, NY, 1998), 4th edn.

[22] I. Barin, *Thermochemical Data of Pure Substances* (VCH, Weinheim, 1995), 3rd edn.

[23] D. D. Wagman, W. H. Evans, V. B. Parker, R. H. Schumm, I. Halow, S. M. Bailey, K. L. Churney, and R. L. Nuttall, *The NBS tables of chemical thermodynamic properties*, J. Phys. Chem. Ref. Data **11**, Supplement No. 2 (1982).

[24] W. Kohn and L. J. Sham, *Self-consistent equations including exchange and correlation effects*, Phys. Rev. **140**, A1133 (1965).

[25] U. von Barth and L. Hedin, *A local exchange-correlation potential for the spin polarized case: I*, J. Phys. C: Solid State Phys. **5**, 1629 (1972).

[26] J. P. Perdew, K. Burke, and M. Ernzerhof, *Generalized Gradient Approximation Made Simple*, Phys. Rev. Lett. **77**, 3865–3868 (1996).

[27] Y. Zhang, D. A. Kitchaev, J. Yang, T. Chen, S. T. Dacek, R. A. Sarmiento-Pérez, M. A. L. Marques, H. Peng, G. Ceder, J. P. Perdew, and J. Sun, *Efficient first-principles prediction of solid stability: Towards chemical accuracy*, npj Comput. Mater. **4**, 9 (2018).

[28] E. B. Isaacs and C. Wolverton, *Performance of the strongly constrained and appropriately normed density functional for solid-state materials*, Phys. Rev. Materials **2**, 063801 (2018).

[29] J. Wellendorff, K. T. Lundgaard, K. W. Jacobsen, and T. Bligaard, *mBEEF: An accurate semi-local Bayesian error estimation density functional*, J. Chem. Phys. **140**, 144107 (2014).

[30] J. Sun, A. Ruzsinszky, and J. P. Perdew, *Strongly Constrained and Appropriately Normed Semilocal Density Functional*, Phys. Rev. Lett. **115**, 036402 (2015).

[31] M. Pandey and K. W. Jacobsen, *Heats of formation of solids with error estimation: The mBEEF functional with and without fitted reference energies*, Phys. Rev. B **91**, 235201 (2015).

[32] J. Yan and J. K. Nørskov, *Calculated formation and reaction energies of 3d transition metal oxides using a hierarchy of exchange-correlation functionals*, Phys. Rev. B **88**, 245204 (2013).

[33] S.-L. Shang, Y. Wang, T. J. Anderson, and Z.-K. Liu, *Achieving accurate energetics beyond (semi-)local density*

functional theory: Illustrated with transition metal disulfides, Cu_2ZnSnS_4, and Na_3PS_4 related semiconductors, Phys. Rev. Materials **3**, 015401 (2019).

[34] J. Yan, J. S. Hummelshøj, and J. K. Nørskov, *Formation energies of group I and II metal oxides using random phase approximation*, Phys. Rev. B **87**, 075207 (2013).

[35] T. S. Jauho, T. Olsen, T. Bligaard, and K. S. Thygesen, *Improved description of metal oxide stability: Beyond the random phase approximation with renormalized kernels*, Phys. Rev. B **92**, 115140 (2015).

[36] T. Olsen, C. E. P., J. E. Bates, A. Ruzsinszky, and K. S. Thygesen, *Beyond the RPA and GW methods with adiabatic xc-kernels for accurate ground state and quasiparticle energies*, npj Comput. Mater. **5**, 106 (2019).

[37] M. Pozzo and D. Alfé, *Structural properties and enthalpy of formation of magnesium hydride from quantum Monte Carlo calculations*, Phys. Rev. B **77**, 104103 (2008).

[38] G. Mao, X. Hu, X. Wu, Y. Dai, S. Chu, and J. Deng, *Benchmark Quantum Monte Carlo calculation of the enthalpy of formation of MgH2*, Int. J. of Hydrogen Energy **36**, 8388–8391 (2011).

[39] S. Grindy, B. Meredig, S. Kirklin, J. E. Saal, and C. Wolverton, *Approaching chemical accuracy with density functional calculations: Diatomic energy corrections*, Phys. Rev. B **87**, 075150 (2013).

[40] Y. Yu, M. Aykol, and C. Wolverton, *Reaction thermochemistry of metal sulfides with GGA and GGA+U calculations*, Phys. Rev. B **92**, 195118 (2015).

[41] M. Aykol and C. Wolverton, *Local environment dependent GGA+U method for accurate thermochemistry of transition metal compounds*, Phys. Rev. B **90**, 115105 (2014).

[42] C. J. Bartel, S. L. Millican, A. M. Deml, J. R. Rumptz, W. Tumas, A. W. Weimer, S. Lany, V. Stevanović, C. B. Musgrave, and A. M. Holder, *Physical descriptor for the Gibbs energy of inorganic crystalline solids and temperature-dependent materials chemistry*, Nat. Commun. **9**, 4168 (2018).

[43] O. Levy, G. L. W. Hart, and S. Curtarolo, *Structure maps for hcp metals from first-principles calculations*, Phys. Rev. B **81**, 174106 (2010).

[44] O. Levy, M. Jahnátek, R. V. Chepulskii, G. L. W. Hart, and S. Curtarolo, *Ordered Structures in Rhenium Binary Alloys from First-Principles Calculations*, J. Am. Chem. Soc. **133**, 158–163 (2011).

[45] S. Curtarolo, W. Setyawan, G. L. W. Hart, M. Jahnátek, R. V. Chepulskii, R. H. Taylor, S. Wang, J. Xue, K. Yang, O. Levy, M. J. Mehl, H. T. Stokes, D. O. Demchenko, and D. Morgan, *AFLOW: An automatic framework for high-throughput materials discovery*, Comput. Mater. Sci. **58**, 218–226 (2012).

[46] K. Yang, C. Oses, and S. Curtarolo, *Modeling Off-Stoichiometry Materials with a High-Throughput Ab-Initio Approach*, Chem. Mater. **28**, 6484–6492 (2016).

[47] A. R. Supka, T. E. Lyons, L. S. I. Liyanage, P. D'Amico, R. Al Rahal Al Orabi, S. Mahatara, P. Gopal, C. Toher, D. Ceresoli, A. Calzolari, S. Curtarolo, M. Buongiorno Nardelli, and M. Fornari, *AFLOWπ: A minimalist approach to high-throughput ab initio calculations including the generation of tight-binding hamiltonians*, Comput. Mater. Sci. **136**, 76–84 (2017).

[48] G. Kresse and J. Furthmüller, *Efficient iterative schemes for ab initio total-energy calculations using a plane-wave basis set*, Phys. Rev. B **54**, 11169–11186 (1996).

[49] C. E. Calderon, J. J. Plata, C. Toher, C. Oses, O. Levy, M. Fornari, A. Natan, M. J. Mehl, G. L. W. Hart, M. Buongiorno Nardelli, and S. Curtarolo, *The AFLOW standard for high-throughput materials science calculations*, Comput. Mater. Sci. **108 Part A**, 233–238 (2015).

[50] M. A. Blanco, E. Francisco, and V. Luaña, *GIBBS: isothermal-isobaric thermodynamics of solids from energy curves using a quasi-harmonic Debye model*, Comput. Phys. Commun. **158**, 57–72 (2004).

[51] C. Toher, J. J. Plata, O. Levy, M. de Jong, M. Asta, M. Buongiorno Nardelli, and S. Curtarolo, *High-throughput computational screening of thermal conductivity, Debye temperature, and Grüneisen parameter using a quasiharmonic Debye model*, Phys. Rev. B **90**, 174107 (2014).

[52] C. Toher, C. Oses, J. J. Plata, D. Hicks, F. Rose, O. Levy, M. de Jong, M. Asta, M. Fornari, M. Buongiorno Nardelli, and S. Curtarolo, *Combining the AFLOW GIBBS and elastic libraries to efficiently and robustly screen thermomechanical properties of solids*, Phys. Rev. Materials **1**, 015401 (2017).

[53] H. Kageyama, K. Hayashi, K. Maeda, J. P. Attfield, Z. Hiroi, J. M. Rondinelli, and K. R. Poeppelmeier, *Expanding frontiers in materials chemistry and physics with multiple anions*, Nat. Commun. **9**, 772 (2018).

[54] P. Giannozzi *et al.*, *QUANTUM ESPRESSO: a modular and open-source software project for quantum simulations of materials*, J. Phys.: Condens. Matter **21**, 395502 (2009).

[55] V. Blum, R. Gehrke, F. Hanke, P. Havu, V. Havu, X. Ren, K. Reuter, and M. Scheffler, *Ab initio molecular simulations with numeric atom-centered orbitals*, Comput. Phys. Commun. **180**, 2175–2196 (2009).

[56] X. Gonze *et al.*, *First-principles computation of material properties: the ABINIT software project*, Comput. Mater. Sci. **25**, 478–492 (2002).

[57] *The ELK Code:* http://elk.sourceforge.net/ (2020). (accessed January 6, 2021).

[58] S. R. Hall, F. H. Allen, and I. D. Brown, *The Crystallographic Information File (CIF): a New Standard Archive File for Crystallography*, Acta Crystallogr. Sect. A **47**, 655–685 (1991).

[59] R. H. Taylor, F. Rose, C. Toher, O. Levy, K. Yang, M. Buongiorno Nardelli, and S. Curtarolo, *A RESTful API for exchanging materials data in the AFLOWLIB.org consortium*, Comput. Mater. Sci. **93**, 178–192 (2014).

[60] F. Rose, C. Toher, E. Gossett, C. Oses, M. Buongiorno Nardelli, M. Fornari, and S. Curtarolo, *AFLUX: The LUX materials search API for the AFLOW data repositories*, Comput. Mater. Sci. **137**, 362–370 (2017).

[61] D. Hicks, C. Oses, E. Gossett, G. Gomez, R. H. Taylor, C. Toher, M. J. Mehl, O. Levy, and S. Curtarolo, *AFLOW-SYM: platform for the complete, automatic and self-consistent symmetry analysis of crystals*, Acta Crystallogr. Sect. A **74**, 184–203 (2018).

[62] C. Oses, E. Gossett, D. Hicks, F. Rose, M. J. Mehl, E. Perim, I. Takeuchi, S. Sanvito, M. Scheffler, Y. Lederer, O. Levy, C. Toher, and S. Curtarolo, *AFLOW-CHULL: Cloud-Oriented Platform for Autonomous Phase Stability Analysis*, J. Chem. Inf. Model. **58**, 2477–2490 (2018).

[63] L. C. Allen, *Electronegativity Is the Average One-Electron Energy of the Valence-Shell Electrons in Ground-State Free Atoms*, J. Am. Chem. Soc. **111**, 9003–9014 (1989).

[64] J. B. Mann, T. L. Meek, and L. C. Allen, *Configuration Energies of the Main Group Elements*, J. Am. Chem. Soc. **122**, 2780–2783 (2000).

[65] J. B. Mann, T. L. Meek, E. T. Knight, J. F. Capitani, and L. C. Allen, *Configuration Energies of the d-Block Elements*, J. Am. Chem. Soc. **122**, 5132–5137 (2000).

[66] E. Fluck and K. G. Heumann, *Periodensystem der Elemente* (Wiley-VCH, Weinheim, 2012), 5th edn.

[67] A. L. Allred and E. G. Rochow, *A scale of electronegativity based on electrostatic force*, J. Inorg. Nucl. Chem. **5**, 264–268 (1958).

[68] P. Karen, P. McArdle, and J. Takats, *Toward a comprehensive definition of oxidation state (IUPAC Technical Report)*, Pure Appl. Chem. **86**, 1017–1081 (2014).

[69] P. Karen, P. McArdle, and J. Takats, *Comprehensive definition of oxidation state (IUPAC Recommendations 2016)*, Pure Appl. Chem. **88**, 831–839 (2016).

[70] L. Pauling, *The nature of the chemical bond. IV. The energy of single bonds and the relative electronegativity of atoms*, J. Am. Chem. Soc. **54**, 3570–3582 (1932).

[71] G. Henkelman, A. Arnaldsson, and H. Jónsson, *A fast and robust algorithm for Bader decomposition of charge density*, Comput. Mater. Sci. **36**, 354–360 (2006).

[72] C. M. Rost, E. Sachet, T. Borman, A. Moballegh, E. C. Dickey, D. Hou, J. L. Jones, S. Curtarolo, and J.-P. Maria, *Entropy-stabilized oxides*, Nat. Commun. **6**, 8485 (2015).

[73] P. Sarker, T. Harrington, C. Toher, C. Oses, M. Samiee, J.-P. Maria, D. W. Brenner, K. S. Vecchio, and S. Curtarolo, *High-entropy high-hardness metal carbides discovered by entropy descriptors*, Nat. Commun. **9**, 4980 (2018).

[74] M. J. Mehl, D. Hicks, C. Toher, O. Levy, R. M. Hanson, G. L. W. Hart, and S. Curtarolo, *The AFLOW Library of Crystallographic Prototypes: Part 1*, Comput. Mater. Sci. **136**, S1–S828 (2017).

[75] D. Hicks, M. J. Mehl, E. Gossett, C. Toher, O. Levy, R. M. Hanson, G. L. W. Hart, and S. Curtarolo, *The AFLOW Library of Crystallographic Prototypes: Part 2*, Comput. Mater. Sci. **161**, S1–S1011 (2019).